The Role of Initial and Final States in Molecular Spectroscopies

Journal:	*Physical Chemistry Chemical Physics*
Manuscript ID	CP-PER-11-2018-007318.R1
Article Type:	Perspective
Date Submitted by the Author:	30-Apr-2019
Complete List of Authors:	Kirchhuebel, Tino; Friedrich Schiller University Jena, Institute of Solid State Physics Monti, Oliver; The University of Arizona, Chemistry and Biochemistry Munakata, Toshiaki; Osaka University, Graduate School of Science, Department of Chemistry Kera, Satoshi; Institute for Molecular Science, Department of Photo-Molecular Science Forker, Roman; Friedrich Schiller University Jena, Department of Physics and Astronomy Fritz, Torsten; Friedrich-Schiller-Universität Jena, Institute of Solid State Physics

PCCP

PERSPECTIVE

The Role of Initial and Final States in Molecular Spectroscopies

Tino Kirchhuebel,*[a] Oliver L. A. Monti [b,c], Toshiaki Munakata [d], Satoshi Kera [e], Roman Forker [a] and Torsten Fritz [a]

Received 00th January 20xx,
Accepted 00th January 20xx

DOI: 10.1039/x0xx00000x

www.rsc.org/

Interpreting experimental spectra of thin films of organic semiconductors is challenging, and understanding the relationship between experimental data obtained by different spectroscopic techniques requires a careful consideration of the initial and final states for each process. The discussion of spectroscopic data is frequently mired in confusion that originates in overlapping terminology with however distinct meaning in different spectroscopies. Here, we present a coherent framework that is capable of treating on equal footing most spectroscopies commonly used to investigate thin films of organic semiconductors. We develop a simple model for the expected energy level positions, as obtained by common spectroscopic techniques, and relate them to the energies of molecular states. Molecular charging energies in photoionization processes, as well as adsorption energies and the screening of molecular charges due to environmental polarization, are taken into account as the main causes for shifts of the measured spectroscopic features. We explain the relationship between these quantities, as well as with the transport gap, the optical gap and the exciton binding energy. Our considerations serve as a model for weakly interacting systems, e.g., various organic molecular crystals, where wave function hybridizations between adjacent molecules are negligible.

Introduction

Understanding the properties of thin films of small organic molecules is important for tailoring materials to the demands of organic-based applications, such as light-emitting diodes (OLEDs), photovoltaic devices (OPVDs), and field-effect transistors (OFETs).[1-5] A thorough characterization requires the use of various complementary experimental techniques. However, the coherent interpretation of the different types of spectroscopic results from these methods is challenging since many different effects must be considered.

Our Perspective provides a framework to understand and interpret the results of different experimental spectroscopies used to probe organic thin films. There is a clear need for the development of such a coherent framework which regards the measurement process itself and the associated initial and final states. This is essential if spectroscopy is to guide rational design of organic electronic devices.Small organic molecules represent a quantum system, consisting of few atomic nuclei and a countable number of electrons, confined to a finite spatial area. Adding or removing an electron, as is done in some of the most common spectroscopic approaches to characterize organic semiconductors, has a significant impact on the overall interactions and energetics in these systems. As a consequence, the molecules relax and take on a new electronic structure. Taking such perturbations by the measurement processes into account is especially important when comparing results from different types of spectroscopies, since different states (anionic, neutral, or cationic) may be probed in different spectroscopies, rendering interpretation of the results anything but straightforward.

Here, we consider effects to be expected from different variants of photoelectron spectroscopies and optical spectroscopy, since these constitute the most widely used methods to study thin films of organic molecules. The energies of the lowest occupied molecular orbital (LUMO), measured in two-photon photoemission (2PPE) and inverse photoelectron spectroscopy (IPES), for example, can differ by as much as 1 eV.[6, 7]

We develop a clear, consistent, and simple model that explains the physical origins of such discrepancies, differentiating what can be learnt from the various experimental approaches. This model establishes relationships between different physical effects and their influence on the energetic positions of spectroscopic features. While most of the ingredients are already known separately, we aim in the present article to put everything into a coherent, consistent and uniform framework. We identify on-site Coulomb energies, which are similar to classical charging energies, as the main reason for apparent discrepancies between the measured energies of the different spectroscopies. In our model we will use the term “charging energies” for them to emphasize their physical origin, as also used by others.[8, 9] These are closely related to the on-site Coulomb Energy U in the Hubbard model,[7, 10, 11] where $U = E_C^+$

[a] Institute of Solid State Physics, Friedrich Schiller University Jena, Helmholtzweg 5, 07743 Jena, Germany
[b] Department of Chemistry and Biochemistry, University of Arizona, 1306 E. University Blvd., Tucson, Arizona 85721, USA
[c] Department of Physics, University of Arizona, 1118 E. Fourth Street, Tucson, Arizona 85721, USA
[d] Department of Chemistry, Graduate School of Science, Osaka University, Toyonaka 560-0043, Japan
[e] Institute for Molecular Science (IMS), National Institutes of Natural Sciences, and SOKENDAI, Okazaki 444-8585, Japan

$+E_C^-$ within the framework of our model. Further, the role and the nature of the molecular initial and final states involved in the various spectroscopic processes will be addressed in detail as they are crucial for the interpretation of the measurement results.

A universal model for the spectroscopy of organic thin films is, however, challenging to formulate, for several reasons. Besides the spectroscopic processes themselves, the molecular environment has a strong influence on the measured spectra. The electronic properties and the optical absorption of molecules within films are strongly altered compared to isolated molecules in the gas phase, due to molecule-molecule and molecule-substrate interactions. Typically, a variety of different interaction mechanisms contribute to the thin film properties: Wave function hybridization and band dispersion, charge transfer between a conductive substrate and the molecular adsorbate, polarization and screening, as well as excitonic coupling. As there are various superimposed effects that may even influence each other, a particular interaction mechanism can often not be studied separately.

Fortunately, in many cases organic molecules interact only weakly with their environment, predominantly through van der Waals forces, as well as electrostatic forces. Our model focuses on such weakly interacting molecular films. These represent ideal model systems since they are affected by a smaller number of different interaction mechanisms that can be disentangled more conveniently. The molecular wave functions can then be approximated by the orbitals of isolated monomers, only weakly perturbed by the environmental interactions, as far as the shape and especially the localization on a single molecule are concerned. Moreover, these weakly interacting systems react especially sensitively to measurement-induced perturbations.

Spectroscopic processes can induce rather strong interactions, e.g., through the generation of electrostatic monopole fields (first order approximation) which polarize the environment. Thus, the charging energies and, consequently, the energies of spectroscopic molecular features depend very sensitively on the environmental polarizability. Comparing IPES and 2PPE, for example, this polarization effect can cause an energy shift of the corresponding unoccupied levels into opposite directions with increasing molecular film thickness, an observation that may appear confusing at first glance.

At the heart of the problem is the common use of the language of single-particle orbitals for the explanation of spectroscopic features stemming from many-body objects (molecules). Our model is based on transitions between quantum mechanical states instead, and we explain how to establish a corresponding single-particle view which resolves common misconceptions and errors. For this purpose a new labeling scheme for experimentally determined features is presented, further developing ideas discussed by Zhu[12]. This scheme does not only account for the altered electron configuration, i.e., the orbital probed, but also for the initial and final (charge) state resulting from the measurement process.This perspective is organized as follows. In the beginning, we discuss the underlying principles of our model, starting with the initial and final states of spectroscopic processes. We further present a way to consistently incorporate these processes into two equivalent types of diagrams - state diagrams and energy level diagrams. At the end of this section the weak interaction limit, required for the applicability of our model, is defined. The second section introduces the concept of charging energies caused by perturbative effects of the measurement processes as the origin for energetic shifts of the measured states and energy levels, and explains their relationship to the exciton binding energy. In the third section, the influence of environmental effects such as polarization or integer charge transfer on states, energy levels, the transport gap and the optical gap is discussed. Subsequently, other effects which should be considered for the interpretation of spectroscopic data but are not included in the present state of our model, are discussed. We finish this perspective with a summary of the main ideas, drawing conclusions about the importance of our model.

Fundamentals and Definition of Terms in the Model

In this section, we explain the underlying principles and assumptions of our model and discuss its limitations. We present a systematic approach for creating state diagrams and related energy level diagrams in a consistent way.

Initial and Final States in Different Spectroscopies

Any spectroscopic process, such as ionization, photon absorption or emission, represents a perturbation of the molecular quantum system. The latter is fully characterized by a *state*, which is a many-body wave function, representing all electrons and nuclei of the probed molecule, as well as each particle that interacts with them. A spectroscopic process initiates a transition from an *initial state*, which existed before the process took place, to a *final state*.

As will become clear throughout this perspective, the initial and final states of spectroscopic processes have a strong impact on the energetic positions of the corresponding spectral features.[14, 15] Thus, considering these states is crucial for the interpretation of such spectra, and, in particular, for the comparison of data obtained from different spectroscopic techniques. Here, we will focus on four different experimental methods: ultraviolet photoelectron spectroscopy (UPS), inverse photoelectron spectroscopy (IPES), optical spectroscopies, and two-photon photoelectron spectroscopy (2PPE). All four are among the most important techniques for measuring occupied and unoccupied molecular levels, the transport gap, the optical gap, the exciton binding energy, as well as other properties of molecules in the gas phase, solution, or thin films. We briefly summarize the outcome of each of these spectroscopic techniques in what follows.

Fig. 1 provides an overview over the possible initial and final states of the key spectroscopic processes of the four experimental techniques. Since the UPS, IPES and optical spectroscopy processes are discussed thoroughly in the literature,[15-23] we will not explain them in detail here. An often

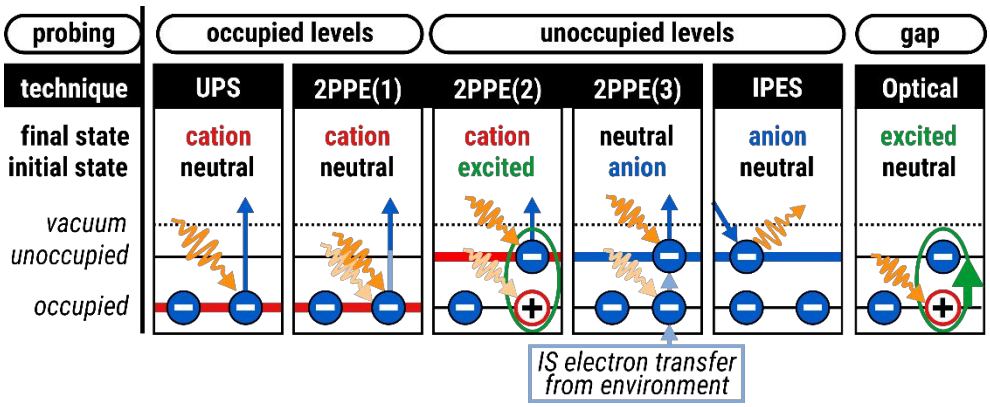

Figure 1 - Simplified scheme of the typical spectroscopic processes in UPS, 2PPE, IPES, and optical spectroscopies in relation to their initial and final states. Thick lines represent the types of energy levels which are probed in the particular processes, and their color coding refers to the molecular state which is most significant with respect to the measured energy of the spectroscopic feature (red: cation, blue: anion, black: neutral). This color coding is used throughout this Perspective. Note that for 2PPE the "initial state" in this scheme refers to the probe process only; it is often called "intermediate state" considering the two-step absorption of pump and probe photons.

overlooked but important fact is that UPS and IPES generate (at least temporarily) positively and negatively charged molecules, respectively, while optical spectroscopies (in the absence of charge transfer excitations) leave the molecules in an overall uncharged excited state.[6, 7]

The three different 2PPE processes illustrated in **Fig. 1** may require a more detailed explanation. The characteristic feature of 2PPE is the absorption of two photons, which can be understood as a two-step process: The pump process is often considered as the transition from an initial state to a so-called "intermediate state", and the probe process as the transition from this intermediate state to a final state. In our considerations, we typically refer to the probe process only, and, thus, the intermediate state is equivalent to the use of an initial state throughout this paper.

An exception is the **2PPE(1)** process, where no intermediate state exists. In this case we treat the two-photon absorption as a one-step process. Probing ***occupied levels in 2PPE*** experiments by non-resonant pump-probe-processes (no intermediate state available to match the pump photon energy) is phenomenologically equivalent to UPS. Thus, the process 2PPE(1) will not be explained further, since the only difference to UPS is the absorption of two photons instead of one, and associated selection rules.

The 2PPE processes in the measurement of ***unoccupied levels*** are much more complex and rather difficult to interpret since at least two different excitation channels have to be considered:

2PPE(2) This is the most typical process when unoccupied levels are probed in 2PPE: The pump photon resonantly excites an electron from an occupied molecular level into an unoccupied molecular level. The intermediate state of the two-step 2PPE process is a neutral excited molecule, where an exciton is formed. The probe photon causes the ionization of the excited molecule, and the final state is a molecular cation plus an electron in vacuum.

2PPE(3) This process can only occur for molecules adsorbed on a substrate or within a molecular film: The hole in a formerly occupied level, created by the pump-excitation, is refilled in a charge-transfer process between the environment and the molecule in the intermediate state. Alternatively, an electron can be excited directly from neighboring molecules or the substrate into an unoccupied level of a molecule. In both cases the intermediate state of the two-step 2PPE process is an anion, whereas the final state is a neutral molecule plus an electron in vacuum.

Whether process 2PPE(2) or 2PPE(3) is dominant in spectra of molecular films depends on the energy level alignment as well as on the spatial wave function overlap between the molecules and their environment.

State Diagrams and Energy Level Diagrams

In order to summarize spectroscopic results, most researchers resort to energy level diagrams as the most common language adopted when discussing thin film electronic structure. As explained by Zhu, however, this can be very problematic:[12] Especially when quasi-particles such as excitons or polarons come into play, there is a danger to mix single-particle levels with those of quasi-particles. Without careful consideration, such diagrams may lead to erroneous conclusions.

In contrast, the presentation of spectroscopic data in the form of state diagrams – though less common – is less controversial, and we adopt this approach to discuss what can be learnt from the different spectroscopic methods. Such quantum states describe the full many-body wave function of all particles in the molecule, as well as all particles the molecule is interacting with. Thus, the initial and final states of *any* spectroscopic process can, in principle, be illustrated within one diagram. In a spectroscopic experiment, the energy balance of the particle used to probe the molecule and the particle which is finally detected provides the information about the energy difference between final and initial state. When the initial state is the **ground state (S_0)** and the final state is the electronically relaxed cation with the photoelectron at rest in vacuum, the energy difference is the **ionization energy** $IE(S_0)$. The labelling "S_0" is necessary for a distinction vis-à-vis the **ionization energy** $IE(S_1)$ **of the excited molecular state (S_1)**, accessible in 2PPE experiments. The anion state is located below the ground state, meaning that the energy corresponding to the **electron affinity** $EA(S_0)$ can be gained by accepting an additional electron. In optical absorption spectroscopy, an excited molecular state is

generated from the initial ground state, which requires an energy amount equal to the *optical gap*. The advantage of this kind of scheme is its clarity and correct inclusion of all many-body effects.

One disadvantage of the states view is that the *transport gap*, also referred to as *fundamental gap*, cannot be deduced from this type of diagram. Relating the states picture to the simpler single-particle view is however not entirely straightforward since it is not a priori obvious which molecular orbitals are actually probed in these processes. Both types of diagrams can, nevertheless, be transformed into each other, as long as the transformation keeps the observable energies invariant.[12] These invariants, namely the *EA*s, the *IE*s, as well as the optical gap, appear in the energy balances of spectroscopic processes. Thus, the direction and length (energy difference) of the corresponding vertical arrows have to be equal in both diagrams, as they define how much energy is gained or spent in a specific process. The two pictures are shown side-by-side in **Fig. 2**.

In the energy level diagram, the energies of molecular levels are defined with respect to the **vacuum level** E_{vac}, representing the reference energy, and the corresponding energy differences are the *IE* and *EA* arrows. Each level is labeled as the molecular orbital which is probed in the measurement process. In photoelectron spectroscopies this is the orbital which initially hosted the photoelectron, whereas in inverse photoelectron spectroscopies it is the former unoccupied orbital, which is occupied with the accepted electron in the final state. In the case of 2PPE measurements, it is either an initially unoccupied orbital populated by the pump photon in the intermediate state, or an initially occupied orbital in the case of non-resonant ionization.

However, applying this transformation creates a problem: The LUMO energy has multiple possible definitions. For instance, the IPES process can probe the LUMO; here the corresponding feature occurs at the energy amount of the $EA(\mathrm{S}_0)$ with respect to the vacuum level. Alternatively, the process 2PPE(2) (see **Fig. 1**) measures the LUMO at the amount of $IE(\mathrm{S}_1)$ below E_{vac}. In general, the absolute values of the independent quantities $EA(\mathrm{S}_0)$ and $IE(\mathrm{S}_1)$ are different, generating discrepancies between possible LUMO energies, obtained from different spectroscopic techniques. Similar problems occur for all other unoccupied energy levels, as well as in other spectroscopic techniques not taken into account here.

These considerations make clear that such a simple labeling scheme is not sufficient for the identification of spectroscopic features, and a more elaborate set of labels is necessary instead. This scheme is already applied in **Fig. 2** and will be introduced in detail in the next subsection.

Proposed Labeling Scheme for Energy Levels

Peaks in electronic spectroscopies are commonly labeled using an energy level scheme (HOMO, LUMO etc.).

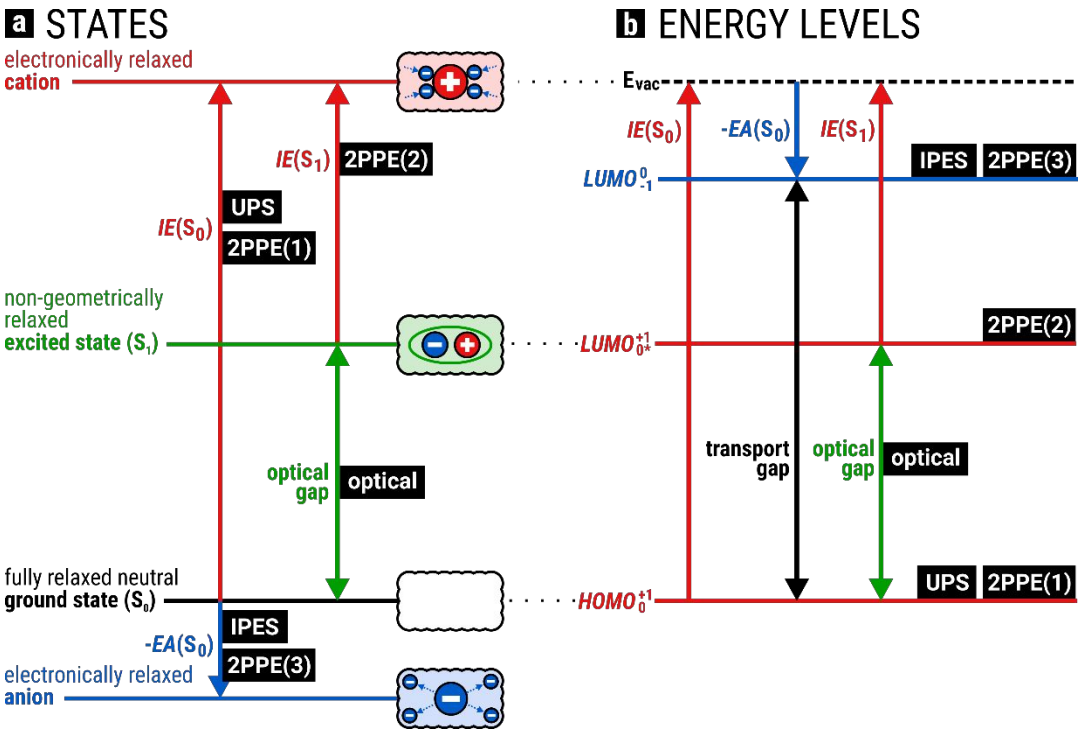

Figure 2 - The relation between multi-particle molecular state diagrams and single-particle electronic energy level diagrams, under the restriction that the occupations of only HOMO and LUMO can be altered. According to Fig. 1, the black boxes link several elements to the spectroscopic processes they can be measured with. (a) The typical order of different molecular states on the scale of their total energies. Any spectroscopic process is represented as a transition between two such states, where the energy differences, represented by arrows, determine the energies of the spectral features. (b) A conversion into the single-particle representation of molecular orbitals must leave these arrows invariant. As one particular molecular orbital may be probed by multiple processes, involving different initial and final states, the corresponding features can appear at several different energies. To distinguish such features, the energy levels are labeled with the initial and final states according to the labeling scheme, introduced in the main text. The color coding refers to the state which mainly determines the energy of the measured level.

Many research reports remain silent on the fact that experimental techniques measure transitions between *states*, from which the energies of particular *orbitals* cannot be extracted unambiguously. This problem is due to the fact that the influence of the measurement process (as detailed below) tends to be ignored. Thus, the spectroscopic transition is better characterized by indicating "initial charge state, final charge state, and altered electron configuration".

In order to provide a consistent framework compatible with the popular single particle language while maintaining the correct physics of transitions and states, we next introduce an extended labeling scheme that includes initial and final states of the probe process, i.e., the process that determines the spectroscopic features, as follows:

$$\mathbf{LEVEL}^{\text{final state of probe process}}_{\text{initial state of probe process}}$$

"**LEVEL**" is to be substituted with **H(OMO), L(UMO), H(OMO)-1**, and so on. The following sub- and superscripts are most common for states in the limit of weak interactions being relevant to organic electronics and assuming integer charges on the molecules: **0** (neutral ground state), **-1** (negatively charged state = anionic state), **+1** (positively charged state = cationic state), **0*** (neutral excited state). We remind the reader that in the case of 2PPE, "initial state" refers to the intermediate state of the 2-step-process after the absorption of the first photon. Even if we use the terms "HOMO" and "LUMO", which contain the word "orbital", the two-fold indexed "levels" in our energy level schemes represent transitions between states in a consistent way, taking care of many-body effects. **Table 1** shows some examples of frequently used labels and their associated spectroscopic transitions.

Note that throughout the paper we will label the energy levels by the names of the orbitals in the *neutral* molecule that they are derived from, in order to avoid confusion. For example, what is called LUMO will actually contain an electron if the state is an anion.

Of course, this labeling scheme does not fully characterize the relevant molecular states: For example, the degree of vibrational excitation is not specified, the complete electronic configuration within a single determinant picture is not indicated, etc. We make the following further assumptions to simplify the discussion in what follows:

i) **The molecule is assumed to be in its neutral ground state geometry**. Within a molecular film, this ground state geometry can, of course, be different from the gas phase geometry. Intermediate and final state nuclear relaxation processes are neglected, and thus the indices "+1" ("-1") indicate that the cation (anion) state involved in the spectroscopic transition is only electronically relaxed. This is justified since often nuclear relaxations are too slow to affect photoemission processes which occur on time-scales of 10^{-15}–10^{-14} s,[24] and in that case only vertical transitions need to be considered.[25]

ii) **In general, the excess hole (excess electron) is assumed to be located in the HOMO (LUMO).** In instances where this is not the case, we use the prime symbol (') to indicate that, e.g., the hole resides in a deeper-lying orbital. For example, $(L_{0^*}^{+1})'$ may indicate a 2PPE process where the excited intermediate state contains an electron in the LUMO and a hole in any level below the HOMO.

Definition of Weakly Interacting Molecular Systems

We finish this introduction of our model by defining the weak interaction limit more explicitly. We define the term "weak interaction" as a perturbative limit, where the electron wave functions can still be reasonably approximated by the unperturbed molecular orbitals. This requires that wave function mixing and non-integer ground state charge transfer between different molecules or between molecules and the substrate are negligible.[26] The model developed below may therefore not be applicable to molecules in strongly hybridized wetting layers on a metal surface. The limitation for the applicability of our model lies in the fact that each molecule must be treatable as a chargeable entity, which is either charge-neutral or contains an *integer* elementary charge.

As the most important consequence and advantage of this limit, there are then well-defined initial and final states, which contain, to a good approximation, integer numbers of elementary charges, and that are essentially molecular in character.

In this limit the single-electron wave functions / orbitals are only slightly altered in shape, and are not strongly energetically broadened by their environment. The gas phase molecular orbitals then provide a suitable basis to describe the molecular levels. Energy renormalization is included, but the formation of electronic bands etc. falls outside the range of weak interactions. Note that screening effects by environmental polarization are, however, included. These may stabilize excess carriers still localized on a charged molecule.

The weak interaction limit is trivially fulfilled by non-interacting isolated monomers in the gas-phase, but it is also realized in molecular films where the molecules interact, e.g., only through van der Waals forces, Coulombic dipole and multipole forces, as well as hydrogen bonds. The spectroscopic features of weakly interacting molecular systems typically consist of rather sharp and often even vibrationally resolved peaks. In contrast, hybridization and covalent bonds, i.e., the mixing of wave functions, fall into the category of strong interactions, beyond the scope of this model. Further, we will not discuss any effects of exciton interactions between neighboring molecules, such as Frenkel exciton coupling or charge transfer excitons,[27] as well as other more exotic effects such as the Kondo effect.

Despite these restrictions, our model is a suitable description for a wide range of molecular films, since most organic molecules form van der Waals bound crystals. The validity holds true for weakly to moderately reactive substrates such as graphite crystals or graphene, various two-dimensional insulators,[28] and even for molecules on metals beyond the wetting layer which are not in direct contact with the substrate surface.[26, 29-32] For molecule-substrate-systems which do not fulfill the preconditions of our model, the insights developed

throughout this manuscript are still valuable: The model provides an understanding of how Coulomb-based effects contribute to the energies of spectral features, even when further effects need to be considered and non-fractional charge transfer needs to be included.

In contrast to the strong interaction limit where charges can be redistributed, e.g., between molecule and surface, the electronic probability density is concentrated in a limited volume (e.g., the dimensions of a molecule) in weakly interacting systems. As a consequence, these systems react very sensitively to external perturbations such as the attachment or

Table 1 - Energy levels, related to different spectroscopic processes, in the denotation of our labeling scheme. The abbreviated forms of H for HOMO and L for LUMO are used.

UPS & 2PPE(1)	Probing the HOMO in UPS	$\boldsymbol{H_0^{+1}}$
IPES	Probing the LUMO in IPES	$\boldsymbol{L_0^{-1}}$
2PPE(2)	Probing the LUMO in 2PPE	$\boldsymbol{L_{0*}^{+1}}$
2PPE(3)	Probing the LUMO in 2PPE (photo-hole quenching in the intermediate state)	$\boldsymbol{L_{0*}^{+1}}$
Optical	Probing the HOMO→LUMO transition through absorption spectroscopy	$\boldsymbol{H_0 \rightarrow L_0^{0*}}$

the ionization of an electron during light–matter interaction. In such cases, the molecules may become charged which is accompanied by additional energy costs or gains.

The weak interaction approximation may of course cause deviations between the model and experimental observations, as a real physical system can rarely be classified as purely weakly interacting. Instead, electronic wave functions show a certain degree of delocalization in the presence of adjacent molecules or a substrate. The individual molecule framework used here is thus neither complete nor entirely accurate. It nevertheless represents a useful framework that enables interpreting molecular spectroscopy in organic thin films.

What is Really Measured? Perturbation by the Measurement Process

Photoemission and optical spectroscopies used to characterize organic thin films do not directly access the molecular ground state, but instead report on transitions between different states. This needs to be treated carefully when interpreting spectroscopic data, in particular by taking into account charging energies.[15] In this section, we will discuss the connection of the specific measurement processes to the observed spectral features. For the sake of simplicity, we start with an isolated molecule and exclude the influence of the environment. In the subsequent section we will add environmental interactions to our considerations.

Charging Energies and the Ground State

The energy level scheme in **Fig. 2** contains two different levels both carrying the term LUMO, namely $\boldsymbol{LUMO_{0*}^{+1}}$ and $\boldsymbol{LUMO_{-1}^{0}}$, indicating clearly the need for a more differentiated nomenclature as proposed here, and a careful consideration of their meanings. We develop next the concept of charging energies, summarized in **Fig. 3**, and use classical electrostatics to explore the difference between the two LUMO-derived levels.

Adding a charge Q to a capacitance C requires an energy of ½ Q^2/C. This is the classical charging energy, and it is ultimately stored in the potential energy of *all* electrons. In the case of molecules which contain a rather small number of electrons, the classical formula is a rather poor quantitative description,

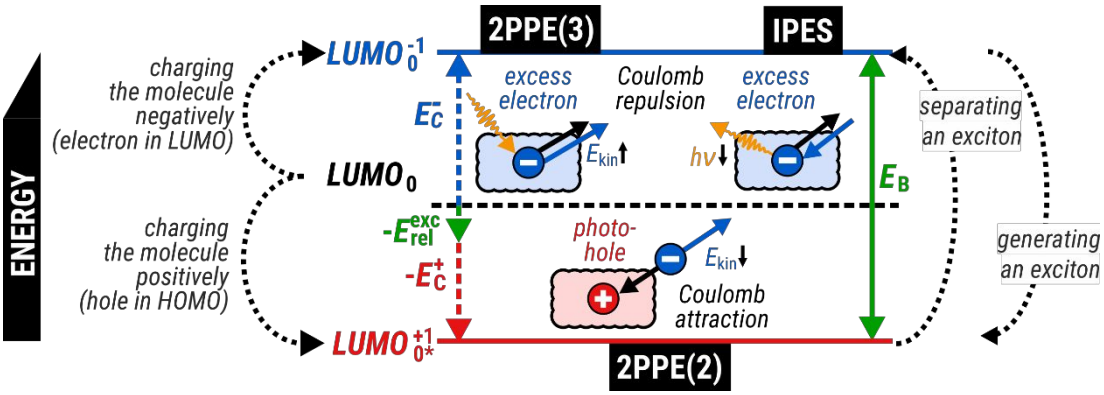

Figure 3 - Energy level scheme of LUMO features, as measurable in different spectroscopic processes. The energy differences are related to their physical origins which are explained in detail in the main text. We denote the ideal energy level of the ground state as $LUMO_0$, while the $LUMO_0^{-1}$ and the $LUMO_{0*}^{+1}$ represent the measurable energies. The energy differences between these levels are mainly originating from the charging energies E_C^+ and E_C^-, and from the considerably smaller excited state relaxation energy $E_{\mathrm{rel}}^{\mathrm{exc}}$. In an alternative representation, these energy contributions can be subsumed to the exciton binding energy E_{B}. The blue arrows inside the small illustrations represent the direction of the electron movement with respect to the directions of Coulomb forces (black arrows). The latter can increase or reduce the kinetic energy $E_{\mathrm{kin}}$of the electron or the photon energy $\mathrm{h}\nu$, as indicated by small black upward or downward arrows behind these quantities.

as electron correlation, exchange and other effects must be taken into account. However, the nature of molecular charging energies can be understood qualitatively based on this classical phenomenon. For instance, according to this expression, aromatic molecules with a larger π-electron system exhibit smaller charging energies, since their effective capacitance is higher. This is born out in most experimental data.[33, 34]

In a *Gedankenexperiment*, we consider the ground state of the neutral molecule as the starting point of the measurement. It is characterized by hypothetical energy levels, labeled with the lower index "0", such as $HOMO_0$ (H_0) and $LUMO_0$ (L_0). To this ground state, charges may be added or subtracted in the course of the measurement, with energetic costs of the charging energies. For example, when attempting to measure the LUMO of the neutral molecule, $LUMO_0$ *(*L_0*)*, an extra electron from the vacuum level may be added to the molecule in an IPES experiment. In an energy level diagram, the energy of the spectroscopic transition is then defined as the energy difference between the vacuum level and the $LUMO_0^{-1}$ level (**Fig. 2b**), where

$$LUMO_0^{-1} = LUMO_0 + E_{C^-} \ . \qquad (1)$$

As a result, one cannot directly observe the energy of the *LUMO*$_0$ orbital associated with the neutral ground state ($EA(\mathrm{S}_0) < (E_{\mathrm{vac}} - LUMO_0)$). The energy required for bringing a molecular electron into vacuum or the energy gain when accepting an electron at rest equals the absolute energy values of the corresponding unperturbed levels with respect to the vacuum level **plus the charging energies** $\boldsymbol{E_C^+}$ **and** $\boldsymbol{-E_{C^-}}$, respectively. For example, if an electron from the vacuum level is transferred to the LUMO in an electron acceptance process, the energy $EA(\mathrm{S}_0) = (E_{\mathrm{vac}} - L_0) - E_{C^-} = E_{\mathrm{vac}} - L_0^{-1}$ is gained.

In general, if either the initial or the final molecular state is an *anion*, the spectroscopic peak corresponds to an energy level at a *higher* energy than the corresponding unperturbed molecular level. Our labeling scheme allows for the interchange of upper and lower indices, without altering the energies of a level in the single-particle picture, as the energy difference between the initial and final states remains the same. For example, $LUMO_0^{-1}$ and $LUMO^0_{-1}$ describe the same energy level in **Fig. 2** and **Fig. 3**, representing an IPES process and a 2PPE(3) process, respectively. In the IPES process, E_{C^-} reduces the energy gain through the electron acceptance, whereas it increases the kinetic energy of the photoelectron in the 2PPE(3) process.

The charging energy E_{C^-} arises from the perturbation by the additional electron, which generates a repulsive potential for all other electrons. The charging energies are thus a measure for the perturbation of the quantum system. Hence, in general the charging energies are larger for smaller molecules and orbitals. Note that we consider here only changes to the occupations of HOMO and LUMO, but the model is easily extendable to other orbitals, as discussed later. The $LUMO_0^{-1}$ level in our terminology equals what is often just referred to as "LUMO" in literature, which is used to define the transport gap.

If the initial or the final molecular state is a *cation*, the spectroscopic peak transforms, within the energy level formalism, into an energy level at a *lower* energy than the corresponding unperturbed molecular level. When the photoelectron in a photoionization process is not bound to the molecule anymore, it is described by a new wave function. It is then not correlated to the rest of the molecular electron system anymore, and the electric field of the atomic nuclei is screened less. In principle, the electron density corresponding to one electron in the former occupied orbital is now missing, and its behavior can be rationalized as a positively charged cloud in the sense of a defect electron (hole). While the photoelectron moves in the attractive potential of the molecular cation it loses kinetic energy. The total energy loss on its way to the detector is the charging energy E_C^+. The $LUMO_{0*}^{+1}$, determined from, e.g., the 2PPE(2)-process, is then observed at an energy of $LUMO_0$ minus E_C^+. The $LUMO_{0*}^{+1}$ corresponds to what is sometimes denoted as *optical LUMO*,[35] owing to the relationship that it can be estimated from the $HOMO_0^{+1}$ plus the optical gap. The $HOMO_0^{+1}$ represents the "HOMO" in typical experimentalist terminology.

In summary, in this *Gedankenexperiment*, each ground state level is located between the corresponding anion and cation levels. The smaller the charging energies, the more closely all levels approach the energies of the ideal ground state levels of the neutral molecule (**Fig. 3**).

Charging Energies and the Exciton Binding Energy

A common but misleading experimental practice is the determination of the "LUMO" energy level from the "HOMO" plus the optical gap. We strongly emphasize that this approach may lead to large errors, since the transport gap and the optical gap are fundamentally different. Instead of the $LUMO_0^{-1}$, which is associated with the transport gap, this procedure actually provides an estimation for the energy of the "optical" $LUMO_{0*}^{+1}$. According to **Fig. 3** the corresponding error equals the sum of the charging energies $(E_C^+ + E_{C^-})$. As explained below, the associated error can be substantial when applied to molecules in a weakly polarizable environment. For molecules in the gas phase, for example, the difference of transport gap minus optical gap can be as large as several eV.

As **Fig. 3** illustrates, the charging energies are directly related to the exciton binding energy of a molecule. We will explore this concept in more detail next.

The exciton binding energy is the energy difference of the transport gap minus the optical gap. The optical gap is just slightly smaller than the H_0-L_0-gap of the unperturbed ground state: Using another *Gedankenexperiment* (see **Appendix A**) where a molecular exciton is separated, one can show that the exciton binding energy is to first-order the sum of the charging energies.[33] The electron in the LUMO of an electronically relaxed excited molecule is therein transferred to a second identical molecule, reaching the final state of an electronically relaxed anion and an electronically relaxed cation. Then, ionizing the excited molecule is actually the same as probing the $LUMO_{0*}^{+1}$, and accepting an excess electron by the second molecule equals the process of probing the $LUMO_0^{-1}$. Thus, the energy difference between the $LUMO_{0*}^{+1}$ and the $LUMO_0^{-1}$ is the exciton binding energy E_B, which has to be spent for the separation of the exciton while the electron is transferred from

the $LUMO_0^{+1}$ to the $LUMO_0^{-1}$. This consideration leads us to the following approximation for the **exciton binding energy E_B:**

$$E_B \approx E_C^+ + E_C^- + E_{rel}^{exc} \quad , \qquad (2)$$

where E_{rel}^{exc} is the **excited state relaxation energy**, which takes the time-dependent nature of optical excitations as well as other relaxation processes originating from the altered electron configuration in the excited state into account.

Environmental Interactions in Molecular Films

A molecule embedded in a film or adsorbed on a substrate experiences forces by interactions with its environment, causing additional shifts of the energy levels, as illustrated in **Fig. 4**. We separate these interaction energies into **permanent interactions w**, which affect the molecular ground state and all other states, and **induced interactions P**, which only occur if the molecule is perturbed externally. In order to distinguish isolated molecules in the gas phase from molecules in a condensed (e.g. adsorbed) state, we label the energy levels of the latter with "*ads*".

In the framework of our model, each energy level can be affected by a total shift of

$$\begin{aligned} \Delta E &= \mp \left(E_C^{\pm} - P^{\pm}\right) - w - E_{rel}^{exc} \\ &= \mp E_{C,eff}^{\pm} - w - E_{rel}^{exc} \end{aligned} \qquad (3)$$

with respect to the energy of the corresponding unperturbed molecular level. Here, $E_C^{\pm}$, $P^{\pm}$, w and E_{rel}^{exc} are typically positive quantities, representing charging energy, polarization energy, permanent interaction energy, and excited state relaxation energy. These are discussed in more detail in the following sections. The positive and negative signs apply for $\left(E_C^- - P^-\right)$ and $\left(E_C^+ - P^+\right)$, respectively. Depending on the respective energy level, some of these quantities can be zero, and positive values of ΔE describe an upward energy shift.

Permanent Interactions

Molecules adsorbed on a substrate or embedded in molecular films are always affected by permanent interactions. Each molecule interacts with adjacent molecules or with the

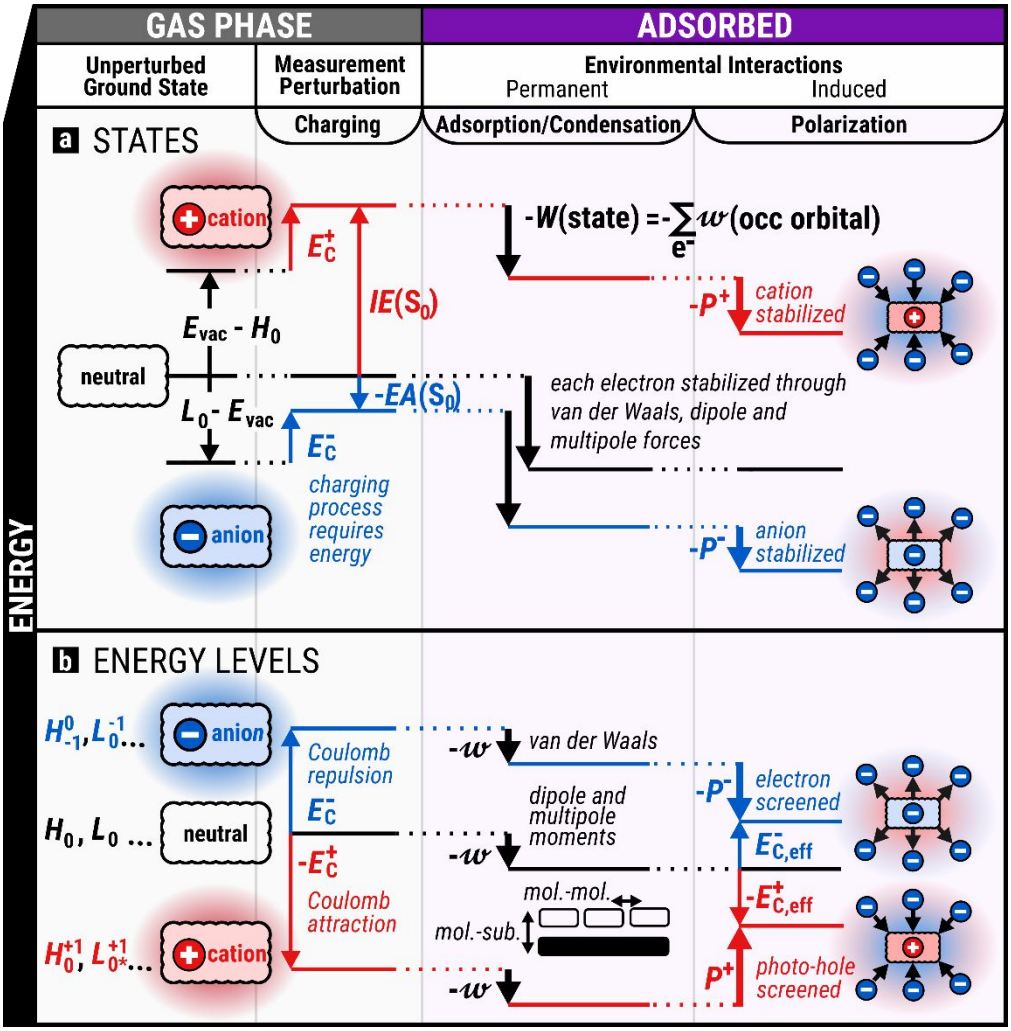

Figure 4 - Influence of permanent (w) and induced (P) environmental interactions on the molecular states (a) and measured energy levels (b). While the charging energies E_C, which destabilize charged states and can cause the energy levels to shift into different energy directions, have the largest impact for molecules in the gas phase, other effects do only occur within a polarizable environment. The permanent interactions w are stabilizing forces, arising from van der Waals or permanent electrostatic forces. They cause down-shifts of all molecular states depending on the number of molecular electrons. In contrast, induced interactions P only occur for charged molecular states which are stabilized as a result of the environmental screening. This reduces the charging energies. E_{rel}^{exc} is not considered here for the sake of simplicity.

substrate through van der Waals forces or permanent electrostatic dipole and multipole moments.

The **total permanent interaction** $W(\text{state})$, which characterizes the adsorption energy of a molecule, contains molecule-substrate and molecule-molecule contributions. For an adsorbed molecule in any particular state this energy is attractive, and $W(\text{state})$ is then defined as a positive quantity, here. This leads to a stabilization of all molecular energy levels and states which are thus shifted to lower energies with respect to the gas phase. However, in a molecular orbital picture each molecular level may shift individually by a different amount of energy, as the molecular orbitals differ in their spatial extent and polarizability. Thus, each electron is affected differently by environmental interactions, which is indicated in our model as an orbital-dependent quantity $\boldsymbol{w}(\text{occupied orbital})$. The total permanent interaction energy of the entire molecular state is then the sum over the interactions of each single electron:

$$W(\text{state}) = \sum_{\substack{\text{all}\\ \text{electrons}}} w(\text{occupied orbital}) \qquad (4)$$

Each molecular state is affected by an individual downward shift $W(\text{state})$ which depends on the particular electron configuration, according to **Eq. (4)**. In compliance with typical adsorption energies this quantity is on the order of several eV for various organic molecules.[36-38]

Note that since HOMO and LUMO typically have similarly extended wave functions, they are expected to experience a similar shift, leading to a rather small difference

$$|w(HOMO) - w(LUMO)| \lesssim 0.1\ eV\ . \qquad (5)$$

For orbitals which are energetically far separated from each other, this is often not the case: Energetically deeper lying levels tend to have a more localized character and thus experience a smaller shift than more spread-out orbitals.

Measurement-Induced Interactions – Polarization

Besides the permanent interactions, some interactions with the molecular environment occur only when the molecular system is externally perturbed. We call this perturbation "measurement-induced interactions": They mainly originate from the ***polarization interactions between a molecule and its environment*** induced during the measurement process, and are labeled $\boldsymbol{P}$.

When a molecule is charged as the result of a spectroscopic process (electron acceptance or photoionization), an electrostatic monopole field is formed around the molecular ion, penetrating and polarizing the environment. In the case of anion formation, electron depletion in the close surroundings generates a positive potential at the location of the negatively charged molecule, stabilizing the anion by P^- relative to an anion in the gas phase. The same is true in the energy level picture, where the extra electron is stabilized.

As polarization energies are typically stabilizing forces, it may seem counterintuitive that P^+ causes an upward shift of energy levels (**Fig. 4**).[39, 40] This is not the case from the viewpoint of the state diagrams, since the total cation energy is also *lowered* by P^+. In contrast, in the single-particle level picture, the *photo-hole* is stabilized, manifesting itself as an upward shift of the *electron* energy level, as the occupation of this hole by an electron becomes energetically less favorable. From an analogous point of view, lifting the hole beyond E_{vac} requires more energy.

From an intuitive view grounded in electrostatics, the polarization energies are reductions of the charging energies: The electric fields arising from the charging energies are the cause, and the environmental polarizations are the effect, counteracting the monopole fields. Due to this causality, the polarization P is assumed to be generally proportional to E_C, while from energy conservation considerations it follows that $|P| \leq |E_\text{C}|$. To emphasize this connection further, we define ***reduced (i.e., effective) charging energies*** $\boldsymbol{E^+_{\text{C,eff}}} = E^+_\text{C} - P^+$ and $\boldsymbol{E^-_{\text{C,eff}}} = E^-_\text{C} - P^-$.

Apart from the value of the charging energies, the polarization energies depend on the interplay between the electric field distribution of the charged molecule and the anisotropic dielectric properties of the environment. Thus, the charge distribution, which can be quite different for anions and cations of the same species, and the molecular packing within a film play, among other factors, a crucial role. P^+ and P^- can, therefore, differ quantitatively.[41]

To summarize (cf. **Table 2**), the neutral ground state levels are simply modified by a shift of $-w$, each. The quantities E_C and P modify only those levels which are probed in spectroscopic transitions, involving differently charged initial and final states. In cases where a neutral excited state is part of the spectroscopic process, e.g., for the measured $LUMO_0^{+1}{}_*$ level, an additional shift E^exc_rel needs to be included.

These examples then represent the rules which must be applied for all measured spectroscopic features: **Spectroscopic features which originate from processes that involve positively (negatively) charged molecular states are generally shifted to lower (higher) energies with respect to the molecular ground state of the isolated molecule.** Based on the assumptions set out above, this is irrespective of whether the charged state constitutes the initial or final state.

Table 2 - Energy shifts ΔE of different energy levels of an adsorbed molecule with respect to the corresponding levels of the ground state of the isolated molecule in the framework of our model. The quantities E^+_C and E^-_C are the charging energies, w denotes the permanent environmental interactions, whereas P^- and P^+ are the measurement-induced polarization energies. The term E^exc_rel is the excited state relaxation energy.

Level	Shift ΔE
$HOMO_0(\text{ads})$	$-w(H)$
$LUMO_0(\text{ads})$	$-w(L)$
$LUMO^0_{-1}(\text{ads})$	$(E^-_\text{C} - P^-) - w(L)$
$HOMO_0^{+1}(\text{ads})$	$-\left(E^+_\text{C} - P^+\right) - w(H)$
$LUMO_0^{+1}{}_*(\text{ads})$	$(E^+_\text{C} - P^+) - w(L) - E^\text{exc}_\text{rel}$

Measurement-Induced Interactions – Charge-Transfer Processes

Due to the practical importance of charge-transfer processes at interfaces, we next consider briefly measurement-induced

charge-transfer processes. We illustrate the salient consequences with the example of a photoionization process.

Typically, a photoelectron interacts with the electric field of the positively charged molecule, and it loses kinetic energy on its way to the detector due to an increase in its potential energy. This is the origin of the charging energy E_C^+. In some circumstances the photo-hole can be quenched by an electron from the environment, neutralizing the molecule and cancelling the electrostatic field. If this occurs on the time-scale of photoemission, one expects to measure an increased kinetic energy,[42] and hence a different binding energy in the energy level diagram. This can be viewed as a reduced charging energy $E_{C,\mathrm{eff}}^+$ due to the charge-transfer process, and in the framework of our model this contribution is included in P^+ and P^-. The quantities P^+ and P^- are large if neutralizing charge-transfer processes are very likely.

Renormalization of Transport Gap, Optical Gap & Exciton Binding Energy

We summarize all these considerations in **Fig. 5** and relate them to the different gaps that are relevant for organic optoelectronics. As shown above, when a molecule is adsorbed on a substrate, both the **transport gap** E_{trans} and the **optical gap** E_{opt} are renormalized, a fact that is also widely reported in the literature.[11, 39, 40, 43-45] Especially for adsorption on metal surfaces, the transport gap narrowing may easily amount to several eV,[46] mainly driven by polarization induced in the substrate and also in adjacent molecules within the film.[39, 40] In addition, one expects also metal-organic wave function hybridization,[30, 47] an aspect that is not treated in our model.

In the simplified model developed in the previous section, the metal surface constitutes a perfectly polarizable medium. Thus, excess charges on a molecule establish an electrostatic monopole field, which can be described by the generation of an image charge inside the metal. The resulting attractive forces lead to a stabilization of the excess charges and, thus, to an upward shift of UPS features and a downward shift of the spectral features in IPES.

Consequently, $HOMO_0^{+1}$ and $LUMO_0^{-1}$ approach each other, narrowing the transport gap by the amount $(P^+ + P^-)$, as illustrated in **Fig. 5 (b)**. This is a consequence of the partial cancellation of the charging energies due to polarization. In the limit of ideal polarization, the minimum transport gap corresponds to the $(LUMO_0 - HOMO_0)$-gap of the molecular ground state, since the excess charges are completely screened by the environment. Within the state diagram in **Fig. 5 (a)**, the cation and anion states are stabilized by P^+ and P^-, respectively, whereas uncharged molecular states are not affected by polarization.

In the framework of our model, we neglect the effect of environmental polarization on optically excited molecular states. Using this approximation, the **optical gap remains constant upon adsorption**. In reality, a polarizable environment also reduces the optical gap, but the reduction is smaller by at least one order of magnitude than for the transport gap. This is estimated from electrostatic considerations, as detailed in **Appendix B**. The underlying physical reason lies in the

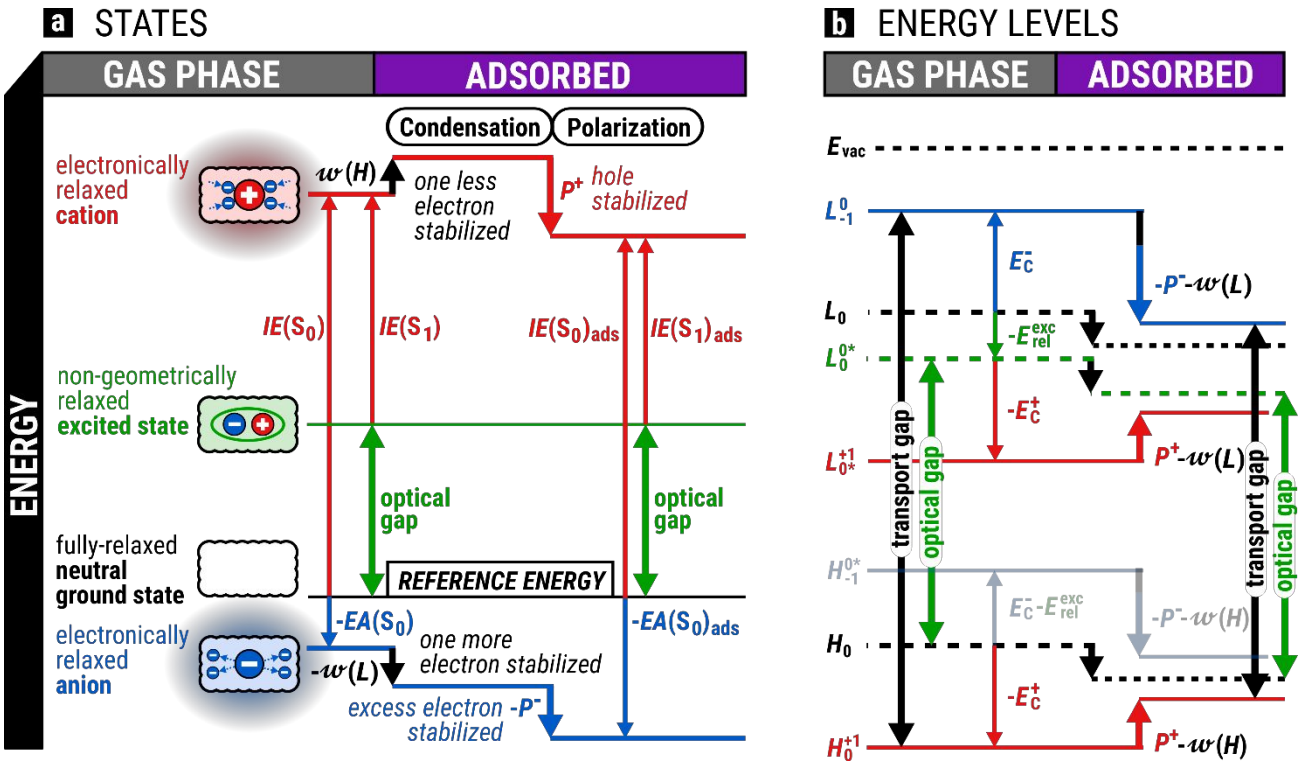

Figure 5 - Complete scheme of (a) molecular states and (b) energy levels within the framework of our model, taking all energy contributions discussed into account. The transport gap narrows in the adsorbed phase, as shown in (b), as a result of the induced interactions P^+ and P^- which reduce the charging energies. As the optical gap remains constant within our approximations, the exciton binding energy decreases. The H_{-1}^{0*} level is illustrated for the sake of completeness only, with reduced saturation. It typically plays a minor role in spectroscopic experiments. Note that (a) and (b) are independent illustrations, neglecting the quantitative connection between the states view and the energy levels picture.

difference of charged final states for measurements of the transport gap vs. neutral excited final states that determine the optical gap. An optically excited state is characterized by the formation of an electron-hole pair, and the resulting oscillating electric dipole interacts much more weakly with the charge density of the environment.[46]

In order to incorporate the optical gap $\boldsymbol{E}_{\mathrm{opt}}$ into the energy level diagram, an additional single-particle energy level has to be defined. We label this new hypothetical level $LUMO_0^{0\,*}$ with an energy

$$LUMO_0^{0\,*} = HOMO_0 + E_{\mathrm{opt}} = LUMO_0 - E_{\mathrm{rel}}^{\mathrm{exc}}\,, \qquad (6)$$

where $E_{\mathrm{rel}}^{\mathrm{exc}}$ is again the excited state relaxation energy. Similar to the ground state level, this level cannot be accessed directly in a measurement process, but its energetic location relative to the ground state $HOMO_0$ can be determined from optical spectroscopies. The meaning of the $LUMO_0^{0\,*}$ originates from the assumption that an excitation of an electron from the HOMO into the LUMO is in many cases a reasonable approximation for an $(S_0{\rightarrow}S_1)$-transition (frozen orbital approximation).

It is important to recognize that the $LUMO_0^{0\,*}$ is not an excitonic level: As the energy level diagram measures the energy of electrons in a single-particle-picture, the $LUMO_0^{0\,*}$ refers exclusively to the energy of the excited electron. As the optically excited state undergoes an electronic relaxation, the $LUMO_0^{0\,*}$ must be located lower in energy than the $LUMO_0$ by $E_{\mathrm{rel}}^{\mathrm{exc}}$. A transition from an excited state to the ground state, where the electron decays back to the HOMO, can be understood as a two-step process in the energy level diagram: The energy $E_{\mathrm{rel}}^{\mathrm{exc}}$ has to be spent in a $LUMO_0^{0\,*}{\rightarrow}LUMO_0$ transition, reversing the excited state relaxation, before a subsequent $LUMO_0{\rightarrow}HOMO_0$ transition can take place. The total energy gain is smaller than the $(LUMO_0 - HOMO_0)$ energy difference.

Compared to the influence of polarization, the impact of permanent interactions on both the transport gap and the optical gap is negligible for a weakly interacting molecule-substrate-system, as $|w(\mathrm{HOMO}) - w(\mathrm{LUMO})|$ is typically one order of magnitude smaller than $(P^+ + P^-)$. Additionally, most energy levels experience a shift in the same direction toward lower energies, originating from w. Thus, we approximate the $(HOMO_0 - LUMO_0)$-gap to be constant upon adsorption from the gas phase:

$$HOMO_0(\mathrm{ads}) - LUMO_0(\mathrm{ads}) \approx HOMO_0 - LUMO_0\,. \qquad (7)$$

In a state diagram, each molecular state of adsorbed molecules is affected by a large downward shift $W(\mathrm{state})$ with respect to the gas phase. For the sake of clarity, this shift is not shown in **Fig. 5.** Instead, the neutral ground state is kept as the constant reference energy, and only the shifts of the other states with respect to this reference energy are illustrated. The extent to which permanent interactions ω manifest themselves in the state diagram is purely the result of excess charges present in anionic and cationic final states, according to **Eq. (4)**.

As a practical summary, we use our model to define expressions that explicitly relate the transport gap and exciton binding energy to different quantities measured by the spectroscopic methods discussed here. In the gas phase this yields:

$$\begin{aligned} E_{\mathrm{trans}} &= LUMO_0^{-1} - HOMO_0^{+1} \\ &= (LUMO_0 + E_{\mathrm{C}}^-) - (HOMO_0 - E_{\mathrm{C}}^+) \\ &= (LUMO_0 - HOMO_0) + (E_{\mathrm{C}}^+ + E_{\mathrm{C}}^-) \end{aligned} \qquad (8)$$

In a polarizable environment for adsorbed molecules, the charging energies are partially compensated by the polarization energies, and the transport gap becomes:

$$\begin{aligned} &E_{\mathrm{trans}}(\mathrm{ads}) = LUMO_0^{-1}(\mathrm{ads}) - HOMO_0^{+1}(\mathrm{ads}) \approx \\ &(LUMO_0(\mathrm{ads}) + E_{\mathrm{C,eff}}^-) - (HOMO_0(\mathrm{ads}) - E_{\mathrm{C,eff}}^+) \\ &\approx (LUMO_0 - HOMO_0) + ((E_{\mathrm{C}}^+ - P^+) + (E_{\mathrm{C}}^- - P^-))\,, \end{aligned} \qquad (9)$$

where the small contribution from possibly different permanent interactions w for the two levels involved is neglected (compare **Eq. (4)**).

The total renormalization of the transport gap upon adsorption can then be expressed as

$$E_{\mathrm{trans}}(\mathrm{ads}) \approx E_{\mathrm{trans}} - (P^+ + P^-)\,, \qquad (10)$$

whereas the optical gap remains approximately constant ($E_{\mathrm{opt}}(\mathrm{ads}) \approx E_{\mathrm{opt}}$). As an obvious result, the environmental polarization reduces the exciton binding energy due to the reduction of the transport gap.[48]

$$\begin{aligned} E_{\mathrm{B}}(\mathrm{ads}) &= E_{\mathrm{trans}}(\mathrm{ads}) - E_{\mathrm{opt}}(\mathrm{ads}) \\ &\approx E_{\mathrm{trans}} - (P^+ + P^-) - E_{\mathrm{opt}} \\ &\approx E_{\mathrm{B}} - (P^+ + P^-) \end{aligned} \qquad (11)$$

Further Effects and Extensions of the Present Model

Our model captures the major effects which determine the energies of spectroscopic features in the weak interaction limit, where charging energies are identified as the main reason for apparent discrepancies between different spectroscopic techniques. Aside from this mechanism, further aspects may have to be considered in practice in order to interpret spectra and compare data from different spectroscopic techniques. We briefly touch on the most important ones below, since they might become important when the particular measurement process exceeds the scope of our model.

Measurement Processes Involving Other Orbitals than HOMO and LUMO.

Although we limit our discussion to changes in the HOMO and LUMO occupations within this Perspective, the principles of this model can be applied to any other transition as well. If a spectroscopic process changes the electron occupation of an orbital $\boldsymbol{HOMO - m}$ ($\boldsymbol{m} \in \mathbf{1,2}$...) at energies lower than the HOMO, or an orbital $\boldsymbol{LUMO + n}$ ($\boldsymbol{n} \in \mathbf{1,2}$...) higher than the LUMO, one can still define charging energies $\boldsymbol{E_C^+}'$ and $\boldsymbol{E_C^-}'$, which represent

the energy difference of the $(\boldsymbol{HOMO-m})_{\boldsymbol{0}}^{\boldsymbol{+1}}-(\boldsymbol{LUMO+n})_{\boldsymbol{0}}^{\boldsymbol{-1}}$-gap minus the optical $(\boldsymbol{HOMO-m})_{\boldsymbol{0}}\rightarrow(\boldsymbol{LUMO+n})_{\boldsymbol{0}}^{\boldsymbol{0}*}$-transition. These charging energies may differ from $\boldsymbol{E_C^+}$ and $\boldsymbol{E_C^-}$, since the latter describe the generation of a hole in the HOMO or an electron in the LUMO, respectively. Further, $\boldsymbol{E_C^{+'}}$ and $\boldsymbol{E_C^{-'}}$ may depend more sensitively on the time scales of the spectroscopic process, since associated holes and electrons possess additional decay channels both within the molecule and toward the environment.

Defining a relationship between the optical gap and the transport gap requires that in both cases the same orbitals are involved. This is, for example, not fulfilled when the transition between the frontier orbitals is forbidden due to selection rules. If the lowest allowed transition is, e.g., $\boldsymbol{HOMO\rightarrow LUMO+1}$, charging energies can be defined as the difference between the optical $\boldsymbol{HOMO_0\rightarrow(LUMO+1)_0^{0*}}$ transition with respect to the energy difference between $\boldsymbol{HOMO_0^{+1}}$ and $\boldsymbol{(LUMO+1)_0^{-1}}$.

In some cases, optical excitations exhibit a strong mixed character, and the corresponding transitions are not sufficiently approximated as transitions between only two molecular orbitals, even in the single particle picture. If the lowest energy optical transition exhibits such a mixed nature, the optical gap and the transport gap, as well as the 2PPE $\boldsymbol{LUMO_{0*}^{+1}}$ (cation final state) and the IPES $\boldsymbol{LUMO_0^{-1}}$ (anion final state), will still be different. One could also define charging energies to account for this difference, which are then less associated with „charging" of the single orbitals, but are more effective ones instead. Additionally, the optical transition cannot be approximated as a simple transition from $\boldsymbol{HOMO_0}$ to $\boldsymbol{LUMO_0^{0*}}$, and one cannot draw initial and final energy levels. Here, one advantage of the „state" picture over the „level" picture becomes clear – ground state and excited state are still well defined concepts.

Site Dependence: Escape Depths, Penetration Depths, and Lateral Area of Probe. Different spectroscopic methods probe different areas and film depths of a sample: The probe volume is determined by the lateral and the vertical resolution. The vertical resolution stems from the finite penetration depths of photons or the limited escape depths of photoelectrons. This has immediate consequences for the energy levels accessed, and the interpretation of the spectroscopically observed transitions. While some spectroscopic techniques mainly probe the surface molecules with an interface to vacuum, other methods probe much more deeply into the molecular film, altering the influence of environmental interactions and screening.

In optical spectroscopies, the penetration depth of the incident light is on the order of 100 nm for organic molecular films and much smaller for highly absorptive metal substrates. In photoelectron spectroscopies (UPS, 2PPE) and IPES the escape depth and the penetration depth of the photoelectrons or the incident electron beam, respectively, strongly depend on the kinetic energy of the electrons and further on the polar angle used in the experiments. UPS experiments with a HeI light source, for example, exhibit escape depths on the order of typically 1-5 molecular monolayers for organic materials, i.e., 0.3 to 1.5 nm.[49] Photoelectron spectroscopies are thus generally more surface sensitive than optical spectroscopic techniques, which must be taken into account for the comparison of the corresponding spectra. Core level spectroscopies – not discussed in any detail in this perspective – typically probe more deeply into the solid than UPS, 2PPE, and IPES.

To complicate matters, the probing volume also reflects e.g. changes in the molecular orientation or conformation as a function of location in the film, affecting the polarization energies, the molecular energy level alignment, or the cross-section in spectroscopic processes.[48, 50-52] Further, depending on the molecular environment, pronounced deformations were reported for various molecules, such as rubrene, PTCDA or F_4TCNQ.[53-56]

Vibrational Structure. The impact of the nuclear degrees of freedom on the spectral appearance may not be negligible, and vibrational features may be observed that can differ between different spectroscopic methods.[42, 53, 57, 58] If the energy resolution of the experimental apparatus prevents the observation of the vibrational structure, a broad asymmetric feature may be measured instead of several distinct maxima, complicating interpretations.

Moreover, it depends on the particular spectroscopic process if the vibrational features appear at the low- or high-energy side of a spectral maximum. In UPS and 2PPE measurements, the vibronic progressions typically appear at the low energy side of the 0-0 transition, whereas the IPES process most commonly generates a vibronic progression at the high-energy side of the 0-0 transition. The intensities of vibrational features further depend on the Franck-Condon factors between the vibrational levels of the initial and final electronic states. As a consequence, no vibronic progression for unoccupied molecular levels was observed, e.g., in recent 2PPE experiments.[59] Note also that the vibrational structures of optical spectra are further influenced by exciton coupling and the formation of H- and J-aggregates.[27] The comparison of features originating from an unoccupied molecular level measured with 2PPE and IPES is a particularly interesting case, since their vibronic progressions are expected to tail toward different sides, and their Franck-Condon Factors may be different. The presence of vibrational features can thus cause an apparent additional peak shift between both techniques even when vibrational transitions are not resolved, simply as a result of spectral broadening, leading to an erroneous interpretation of the magnitude of the shift. Within the approximations of our model, the $LUMO_0^{-1}$ feature and the $LUMO_{-1}^0$ feature are considered to be at equal energies. This is clearly no longer the case when vibrational progressions and relaxation processes are taken into account. This case is related to the comparison of optical absorption and emission spectra, which can be included in an energy level diagram by means of the imaginary levels $LUMO_0^{0*}$ and $LUMO_{0*}^0$. The $LUMO_{0*}^0$ was not discussed previously, but it would appear at slightly lower

energies than the $LUMO_0^{0\,*}$, considering that the Stokes shift may typically reach up to 0.1 eV.

Strong Coupling Regime. The most important restriction in our model is the assumption of the weak interaction limit, and one runs into several challenges when dropping this assumption. We do not intend to extend our model to the strong interaction limit, but highlight the difficulties briefly in the following.

A serious problem is that the initial and final states can no longer be described with isolated molecules that host an integer charge on a particular molecular orbital. The molecule-based single particle picture is therefore harder to apply in such strongly interacting systems. One could of course imagine that electrons are found in a new set of hybrid orbitals that consist of a mixture of wave functions from the interacting partners. In this view, one could still define an integer charge corresponding to the particular molecular state, but the original molecular orbitals are no longer suitable mathematical models. It is then by no means sufficient to label the spectroscopic features according to the names of molecular orbitals, and the nature of the hybrid orbital would have to be specified instead. This is clearly challenging to do and likely less accessible intuitively in all generality.

As a different approach one could consider the charge density projected onto the original orbitals of the isolated molecular ground state instead. In this view, one would end up with partial charges, where the lower and upper indices of our labeling scheme must be fractional numbers. The exact partial charges can hardly be determined and only be accessed by means of theoretical calculations, where the results may strongly differ between the individual calculation methods. They depend sensitively on the interaction strength and the energy level alignment of the interaction partners, profoundly challenging the predictive nature of our simple model.

Extension to Other Spectroscopic Techniques. The applicability of our model is by no means restricted to the spectroscopic techniques at the focus of this perspective. However, each particular spectroscopic process must be considered carefully and in detail if one attempts to extend the model to other methods.

Scanning tunneling spectroscopies (STS) constitute an interesting example. Here, the influence of the tip must be considered explicitly due to the non-negligible bias-induced electric field strength at the location of the molecule. This perturbs the molecular orbitals and may even induce a charge redistribution within the substrate, affecting the polarizability of the latter. Further, the tip and the sample constitute a capacitor whose value differs from the original capacitance of a molecule and its environment. This alters the charging energies significantly and must be taken into account. Apart from these considerations, more exotic many-body effects may influence the tunneling spectra, rendering the case of STS a rather complicated one.

Conclusions

The interpretation of spectroscopic data of organic thin films is a challenging task. Our Perspective provides a coherent framework which captures the inherent differences between various spectroscopic techniques consistently, taking the initial and final states of each measurement process into account, and considering the main physical effects which influence the energetic positions of spectroscopic features.

Each measurement process represents a perturbation of the molecular quantum system. This has a significant impact on the measured energies, complicating a comparison of experimental results among different spectroscopic techniques. Originating from the individual initial and final molecular states, features assigned to one particular molecular orbital can be observed seemingly at different energies in different spectroscopic processes. We thus recommend the use of state diagrams instead of energy level diagrams due to the correct treatment of many-body effects in this view. However, we suggest a labeling scheme for drawing single-particle energy level diagrams to take care of this issue by incorporating the individual initial and final states. This description from the point of view of molecular orbitals is then linked consistently to the full all-electron states representation.

Within our limiting assumption of weak coupling, we present a model for the spectral analysis which provides a consistent interpretation of different spectroscopic methods, lifting the apparent inconsistencies occasionally encountered in the literature. It explains the influence of various perturbative effects on the observed spectroscopic energies arising from the measurement processes and the environment. Taking the initial and final states of spectroscopic processes for the standard techniques of UPS, IPES, 2PPE and optical spectroscopy into account, we discuss the expected differences between the spectroscopic features obtained from these methods.

Our model assumes that the energy level alignment of molecules in the ground state is perturbed by both the measurement processes and the environmental interactions, leading to shifts of the measured energy levels that originate from four different contributions:

i) **Charging energies** ($\boldsymbol{E_C^{\pm}}$), which come into play when a molecule is ionized or accepts an extra electron. They originate from the Coulomb interaction between the excess charge and the other electrons present in the molecule.

ii) **Permanent adsorption energies and condensation energies** ($\boldsymbol{w}$) in molecular films, arising from van der Waals interactions or permanent electrostatic forces.

iii) **Polarization energies** ($\boldsymbol{P^{\pm}}$), arising from the environmental polarization within molecular films and/or the substrate, induced by the electrostatic monopole field of molecular ions.

iv) **Excited state relaxations** ($\boldsymbol{E_{\mathrm{rel}}^{\mathrm{exc}}}$), where the molecular electron system reacts to the altered electron configuration, caused by optical transitions. $E_{\mathrm{rel}}^{\mathrm{exc}}$ does not include relaxations of the atomic nuclei.

Our model reveals the generally different nature of the LUMO feature in IPES and 2PPE measurements, since the processes involve anions and cations, respectively. The principal origin for these differences resides in the charging energies E_C^+ and E_C^- which cause an up- or down-shift of the measured energy levels.

If the measurement process involves a molecular anion state, the energy level will be measured at higher energies. If instead it involves a cation state, the energy level will be measured at lower energies. The exciton binding energy E_{B} is approximately the sum of these charging energies, which thus determine the main difference between optical gap and transport gap.

Further, the measured energies depend strongly on the environmental polarization P, since any screening stabilizes excess charges on the molecule and reduces the charging energies. During film growth or other alterations of the molecular environment, the LUMO in IPES and 2PPE could, for example, shift in different directions. This polarization dependence of the charging energies can narrow the transport gap by several eV in a highly polarizable environment, while the optical gap responds far less sensitively. The exciton binding energy can thus vary in a similar way, depending on the molecular environment.[48]

Van der Waals forces and electrostatic interactions are further stabilizing mechanisms. They also exist in the absence of measurement-induced perturbations, lowering the energy of each molecular energy level individually by an amount $w(\mathrm{occ.\ orbital})$, and accumulating the total adsorption energy $W(\mathrm{state})$ of the many-body state.

We believe that our simplified model is explanatory and establishes a missing link between the many different physical effects that must be considered in spectroscopic experiments, while clearing up some prevalent confusions in the community. It assists the consistent interpretation of spectroscopic data. Finally, the principles of the model can be extended towards other measurement techniques and the inclusion of further physical effects as well.

Appendix A: *Gedankenexperiment* - Relationship Between Charging Energies and Exciton Binding Energy

Fig. A1 illustrates a *Gedankenexperiment*, which clarifies that the exciton binding energy of a molecule is connected to the sum of the charging energies E_{C}^{+} and E_{C}^{-} by a linear scaling law. This *Gedankenexperiment* is inspired by the considerations of Nayak.[33] It uses two identical spatially well separated isolated molecules (A and B) in their ground state as a starting point. Any interactions (Coulomb interactions in particular) between both molecules shall be negligible, preventing the formation of charge-transfer excitons. Nevertheless, a non-zero charge-transfer probability between A and B must be assumed, as two different processes that put A and B in the final state of an electronically relaxed cation and anion, respectively, are considered. The first process is a one-photon absorption, where an electron from the HOMO of molecule A is transferred to the LUMO of molecule B. The second process represents a two-photon absorption, where an electron is excited within molecule A by the first photon, and transferred to B by the second photon. Comparing the energy balance of both processes reveals the relationship between the exciton binding energy and the charging energies within the framework of our model.

One-Photon Absorption

Molecule A absorbs a photon by transferring an electron from its HOMO to the LUMO of molecule B. This process can be broken down into two steps: (i) The ionization of molecule A, undergoing a transition to a cation state. This process is equivalent to probing the $HOMO_0^{+1}$ level in the formalism of our model. (ii) The electron acceptance by molecule B, forming an anion final state, which represents the process of probing the $LUMO_0^{-1}$.

Note that the entire process can be understood as a tunneling mechanism, where (i) and (ii) take place simultaneously, since the electron never has enough energy to reach the vacuum level. The total photon energy, which is required for this process, equals the transport gap E_{trans}:

$$h\nu = L_0^{-1} - H_0^{+1} = E_{\mathrm{trans}} \qquad \text{(A1)}$$

Two-Photon Absorption

The first photon excites an electron from the HOMO into the LUMO of molecule A, where it forms an exciton with the remaining hole in the HOMO, leaving molecule A in the electronically excited state. This represents the process of probing the $LUMO_0^{0^*}$ within the framework of our model, and the energy of the first photon must equal the optical gap E_{opt}:

$$h\nu_1 = L_0^{0^*} - H_0 = E_{\mathrm{opt}} \qquad \text{(A2)}$$

The second photon transfers the electron from the LUMO of molecule A into the LUMO of molecule B, thereby separating the Frenkel exciton. As we neglect any interactions between molecule A and B, no charge transfer exciton is formed. This absorption of the second photon can be separated into two sub-processes: (i) The ionization of molecule A, which induces the transition of molecule A from the S_1 excited state into the cation state. This equals the procedure of probing the $LUMO_{0^*}^{+1}$. (ii) The electron acceptance by molecule B is equivalent to the one-photon absorption process and represents the process of probing the $LUMO_0^{-1}$.

The energy of the second photon must, thus, equal the energy difference between $LUMO_{0^*}^{+1}$ and $LUMO_0^{-1}$:

$$h\nu_2 = L_0^{-1} - L_{0^*}^{+1} = E_{\mathrm{C}}^{+} + E_{\mathrm{C}}^{-} + E_{\mathrm{rel}}^{\mathrm{exc}} \qquad \text{(A3)}$$

Energy Balance and Exciton Binding Energy

As shown in **Fig. A1**, the one-photon process and the two-photon process both induce transitions between exactly the same initial and final states of the two-molecule system. Consequently, the total energy expenditure must be identical:

$$h\nu = h\nu_1 + h\nu_2 \qquad \text{(A4)}$$

Using (A1), (A2) and (A3), this equation transforms to

$$E_{\mathrm{trans}} = E_{\mathrm{opt}} + E_{\mathrm{C}}^{+} + E_{\mathrm{C}}^{-} + E_{\mathrm{rel}}^{\mathrm{exc}} \qquad \text{(A5)}$$

which can be used to find an expression for the exciton binding energy E_{B} within the framework of our model, according to its common definition:

$$E_{\mathrm{B}} = E_{\mathrm{trans}} - E_{\mathrm{opt}} = E_{\mathrm{C}}^{+} + E_{\mathrm{C}}^{-} + E_{\mathrm{rel}}^{\mathrm{exc}} \qquad \text{(A6)}$$

As the charging energies are typically one order of magnitude larger than the excited state relaxation energy, the exciton binding energy can be approximated roughly as the sum of the two charging energies.

$$E_{\mathrm{B}} \approx E_{\mathrm{C}}^{+} + E_{\mathrm{C}}^{-} \qquad \text{(A7)}$$

This *Gedankenexperiment* is implicitly included in **Fig. 3**, containing the following two equivalent points of view explored in Appendix A: Transferring the electron from the excited molecule A to molecule B through the absorption of a second photon requires on the one hand the separation of the exciton, and on the other hand charging molecules A and B positively and negatively, respectively. This is expressed in **Eq. (A7)**.
As the sum of charging energies (A7) are within the framework of our model an equivalent to the on-site Coulomb energy U in the Hubbard model, the Hubbard U is generally expected to be quantitatively very close to the exciton binding energy of a molecule.

Appendix B: Influence of Polarization on Optical Gap and Transport Gap

When molecules are located within a polarizable environment, e.g., surrounded by other molecules or in close distance to a substrate surface, their transport gaps E_{trans} are reduced by the polarization energies $(P^{+} + P^{-})$ [51, 60, 61]

$$\begin{aligned} E_{\mathrm{trans}}(\mathrm{ads}) &= L_0^{-1}(\mathrm{ads}) - H_0^{+1}(\mathrm{ads}) \\ &= IE_0 - EA_0 - (P^{+} + P^{-}) \,, \end{aligned} \qquad \text{(B1)}$$

where (ads) refers to an adsorbed molecular film, whereas IE_0 and EA_0 are the ionization energy and electron affinity, respectively, of the same molecules in the gas phase. The polarization energies are a consequence of the (inverse) photoemission processes in a dielectric environment, creating molecular cations (anions) which polarize the environment mainly due to their electrostatic monopole field.
In contrast, a molecule in an optically excited state is in its entirety still electrically neutral, representing an oscillating

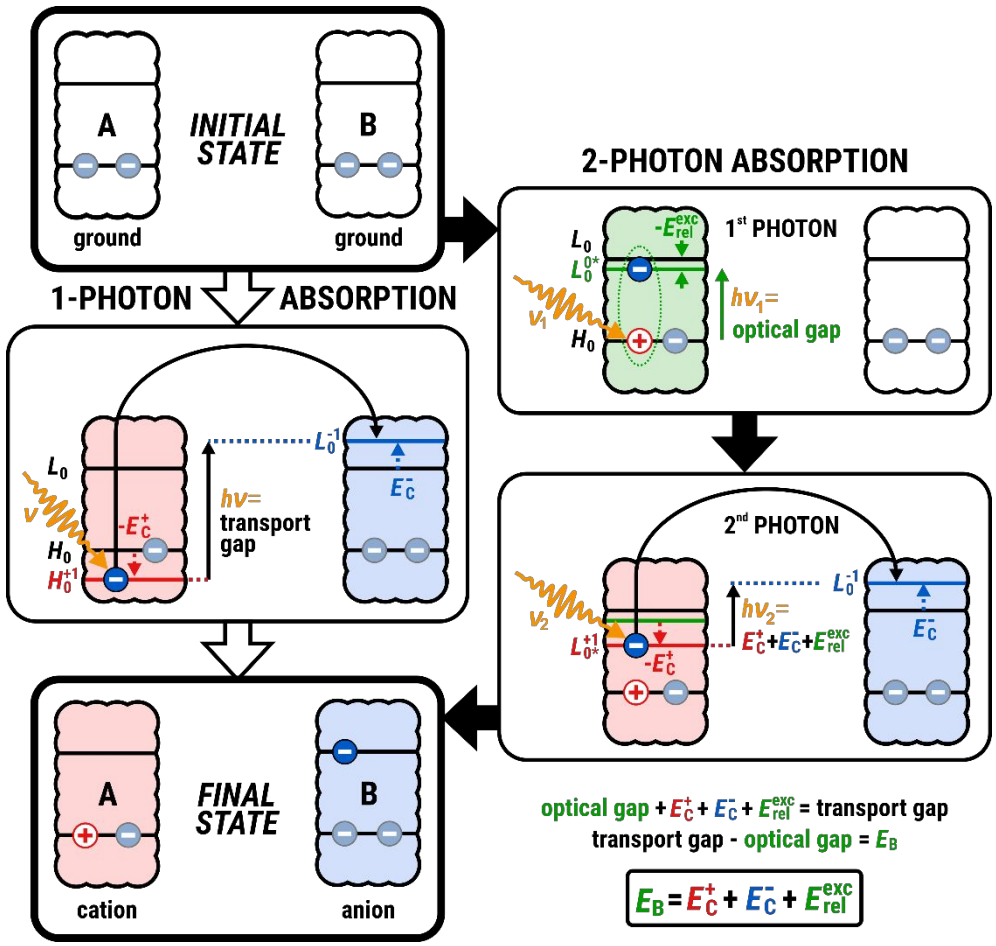

Figure A1 - *Gedankenexperiment* illustrating the relationship between the exciton binding energy E_{B}, the charging energies E_{C}^{+} and E_{C}^{-}, and the excited state relaxation energy $E_{\mathrm{rel}}^{\mathrm{exc}}$. Two non-interacting identical molecules, labeled "A" and "B", undergo a transition from the two-molecule state (A,B) = (ground, ground) to the state (A,B) = (cation, anion), induced by two different photon absorption processes. In the one-photon absorption process, the photoelectron tunnels directly from the HOMO of molecule A to the LUMO of molecule B, whereas in the two-photon absorption process, molecule A is excited by the first photon before the charge transfer process is induced by the absorption of a second photon. The photon energies $h\nu$, $h\nu_1$ and $h\nu_2$, required for these processes, are expressed in the framework of our model. The electrons, drawn with reduced saturation, are just for clarification of the electron configuration, and, as energy conservation reveals, cannot be drawn at these energies in a quantitative energy level diagram.

electric dipole. This dipole polarizes the molecular environment as well, but we neglect this effect on the optical gap in our model. In order to justify this approximation, we present a very simple semi-quantitative estimation how the optical gap and the transport gap are affected by polarization.

For this purpose, we consider a molecular anion or cation (monopole) located within a dielectric medium 1 with relative permittivity ε_1 near the interface of a dielectric medium 2 with permittivity ε_2, and compare it to an optically excited molecule (dipole) at the same position. As illustrated in **Fig. B1**, the charged molecule is roughly approximated as a point charge of Q = -e in vacuum, whereas the excited molecule is approximated as a point dipole $\vec{\mu}$ in our case parallel to the surface. Both Q and $\vec{\mu}$ are located at a distance d to the interface of medium 2. The point charge induces an interface charge within medium 2, and the corresponding electric field at the location of the original charge can be calculated by means of the method of image charges. The charge density within medium 2 is then replaced by an imaginary point charge (image charge)

$$Q' = -\frac{\varepsilon_2 - \varepsilon_1}{\varepsilon_2 + \varepsilon_1} Q \qquad \text{(B2)}$$

at the location $-d$ with respect to the interface, and medium 1 is assumed to be extended infinitely beyond the interface, replacing medium 2. The same method can be applied for the dipole case, where an image dipole

$$\vec{\mu}' = -\frac{\varepsilon_2(\omega_0) - \varepsilon_1(\omega_0)}{\varepsilon_2(\omega_0) + \varepsilon_1(\omega_0)} \vec{\mu} \qquad \text{(B3)}$$

in vacuum at the location $-d$ can be assumed as a substitution for the real charge distribution within medium 2. However, due to the oscillation of the dipole density with the excitation frequency ω_0 of the absorbed electromagnetic wave, the frequency-dependent complex dielectric functions of the dielectric media should be taken into account. The **monopole-monopole interaction energies E_{MM}** between point charge and image charge and the **dipole-dipole interaction energies E_{DD}** between point dipole and image dipole are calculated according to classical electrostatics as

$$E_{\mathrm{MM}} = -\frac{1}{4\pi\varepsilon_0\varepsilon_1} \frac{Q^2}{2d} \frac{\varepsilon_2 - \varepsilon_1}{\varepsilon_2 + \varepsilon_1} \qquad \text{(B4)}$$

$$E_{\mathrm{DD}} = -\frac{1}{4\pi\varepsilon_0 Re(\varepsilon_1(\omega_0))} \frac{\mu^2}{(2d)^3} Re\left(\frac{\varepsilon_2(\omega_0) - \varepsilon_1(\omega_0)}{\varepsilon_2(\omega_0) + \varepsilon_1(\omega_0)}\right) \qquad \text{(B5)}$$

where e is the elementary charge, ε_0 is the vacuum permittivity and μ is the transition dipole moment of the molecular electronic transition.

Modeling a single isolated molecule adsorbed on a substrate, medium 1 is assumed to be vacuum ($\varepsilon_1 = 1$). Using parameters of the well-characterized molecule-substrate system perylene-3,4,9,10-tetracarboxylic dianhydride (PTCDA) on Ag(111), one can estimate the relevant interaction energies. An adsorption height of around 3 Å was reported for PTCDA in contact to the Ag(111) surface, and this value is used as an approximation for d.[62] As also done by Forker *et al.*,[63] the complex dielectric function of silver reported by Babar *et al.* [64] for the frequency ω_0 of the main absorption line of PTCDA ($\lambda = 536$ nm, $\hbar\omega_0 = 2.313$ eV) is used, giving

$$Re\left(\frac{\varepsilon_2(\omega_0) - 1}{\varepsilon_2(\omega_0) + 1}\right) = 1.183\,. \qquad \text{(B6)}$$

In the static limit, ε_2 is assumed to be infinity, leading to

$$E_{\mathrm{MM}} = -\frac{1}{4\pi\varepsilon_0} \frac{e^2}{2d}\,. \qquad \text{(B7)}$$

We will compare the corresponding interaction energies with those of a PTCDA molecule within the second layer, where $d \approx 6$ Å.[63] The literature values for the transition dipole moment of the $S_0 \rightarrow S_1$ transition of PTCDA vary between (6.45 ± 0.70) D and (7.4 ± 0.7) D.[65-67] In the following, we will use an approximate value of 7.0 D for our calculations.

The results are summarized in **Table B1**. E_{MM} is larger than E_{DD} by a factor of 14 for a molecule adsorbed on the substrate surface. Even more strikingly, the difference is almost two orders of magnitude when the distance is doubled. This estimation indicates that the reduction of the measured transport gap of an organic molecule adsorbed on a metal is typically by at least one order of magnitude larger than the reduction of the optical gap. This difference is mainly attributed to the much stronger distance-dependence of dipole-dipole energies than monopole-monopole interaction energies.

A similar behavior is expected for a molecule embedded in a molecular crystal. The surrounding molecules can be approximated as a strongly anisotropic effective medium with

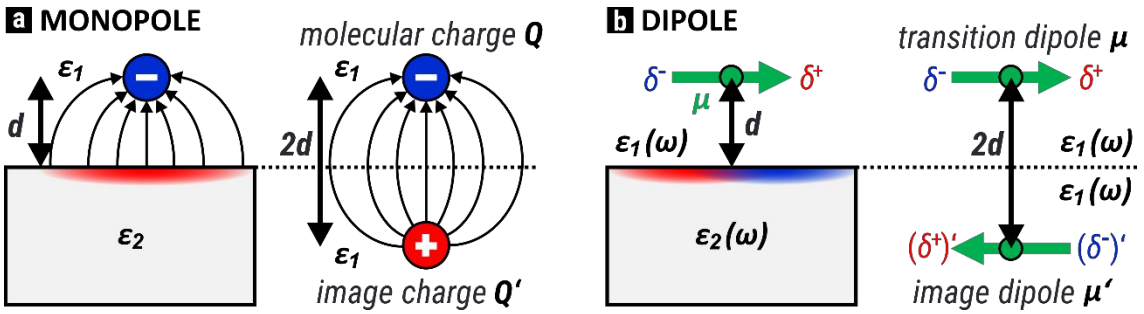

Figure B1 - A charged **(a)** (optically excited **(b)**) molecule, adsorbed on a polarizable substrate, is roughly approximated as a point-charge (dipole) within medium 1 with permittivity ε_1 at a distance d from the interface to another dielectric medium 2 with permittivity ε_2. Inside medium 2 a polarization charge density is generated, creating an electric field at the position of the initial charge (dipole). This field can be calculated by means of the method of image charges as illustrated in the right parts of (a) and (b) and briefly explained in the main text.

more complicated dielectric properties. Nevertheless, an anion or cation exhibits a monopole field which is much stronger than the oscillating dipole field of an excited molecule. The environmental polarization induced by a charged molecule is thus expected to be always significantly stronger than the polarization induced by a molecular exciton, explaining the higher sensitivity of the transport gap to the dielectric environment of a molecule when compared to the optical gap.

Table B1 Monopole-monopole (dipole-dipole) interaction energies E_{MM} (E_{DD}) between a point charge (oscillating point dipole with $\hbar\omega_0 = 2.313$ eV) in vacuum and a mirror charge (mirror dipole) in an ideally polarizable medium, separated by a distance 2d. The dipole orientations are parallel to the surface.

d	E_{MM}	E_{DD}
3 Å	-2.4 eV	-0.17 eV
6 Å	-1.2 eV	-0.02 eV

Conflicts of interest

There are no conflicts to declare.

Acknowledgements

This work was financed by the Deutsche Forschungsgemeinschaft (DFG) grant nos. FO 770/2-1 and FR 875/16-1. T.K. gratefully acknowledges funding by the Evonik Stiftung. O.L.A.M. gratefully acknowledges support from the U.S. National Science Foundation under grant no. CHE-1565497.

References

1. N. Koch, *Chem. Phys. Chem*, 2007, **8**, 1438-1455.
2. S. H. Liu, W. C. M. Wang, A. L. Briseno, S. C. E. Mannsfeld and Z. N. Bao, *Adv. Mater.*, 2009, **21**, 1217-1232.
3. S. Reineke, M. Thomschke, B. Lussem and K. Leo, *Rev. Mod. Phys.*, 2013, **85**, 1245-1293.
4. A. Mishra and P. Bauerle, *Angew. Chem. Int. Ed. Engl.*, 2012, **51**, 2020-2067.
5. I. H. Campbell, S. Rubin, T. A. Zawodzinski, J. D. Kress, R. L. Martin, D. L. Smith, N. N. Barashkov and J. P. Ferraris, *Phys. Rev. B*, 1996, **54**, 14321-14324.
6. M. Marks, S. Sachs, C. H. Schwalb, A. Scholl and U. Hofer, *J. Chem. Phys.*, 2013, **139**, 124701.
7. G. Dutton and X. Y. Zhu, *J. Phys. Chem. B*, 2002, **106**, 5975-5981.
8. E. Abad, C. Gonzalez, J. Ortega and F. Flores, *Org. Electron.*, 2010, **11**, 332-337.
9. E. Abad, J. I. Martinez, J. Ortega and F. Flores, *J. Phys.: Condens. Matter*, 2010, **22**, 304007.
10. J. D. Sau, J. B. Neaton, H. J. Choi, S. G. Louie and M. L. Cohen, *Phys. Rev. Lett.*, 2008, **101**, 026804.
11. I. F. Torrente, K. J. Franke and J. I. Pascual, *J. Phys.: Condens. Matter*, 2008, **20**, 184001.
12. X. Y. Zhu, *J. Phys. Chem. Lett.*, 2014, **5**, 2283-2288.
13. H. Yoshida, K. Yamada, J. Tsutsumi and N. Sato, *Phys. Rev. B*, 2015, **92**, 075145.
14. N. J. Watkins, C. D. Zangmeister, C. K. Chan, W. Zhao, J. W. Ciszek, J. M. Tour, A. Kahn and R. D. van Zee, *Chem. Phys. Lett.*, 2007, **446**, 359-364.
15. D. Cahen and A. Kahn, *Adv. Mater.*, 2003, **15**, 271-277.
16. K. Ozawa, in *Compendium of Surface and Interface Analysis*, ed. T. S. S. S. of Japan, Springer Singapore, Singapore2018, pp. 783-790.
17. M. Pope and C. E. Swenberg, *Electronic processes in organic crystals and polymers*, Oxford University Press1999.
18. W. C. Price, eds. D. R. Bates and B. Bederson, Academic Press1974, vol. 10, pp. 131 - 171.
19. F. Reinert and S. Hüfner, *New J. Phys*, 2005, **7**, 97.
20. A. Damascelli, *Phys. Scr.*, 2004, **T109**, 61-74.
21. N. V. Smith, *Rep. Prog. Phys.*, 1988, **51**, 1227-1294.
22. D. W. Ball, *Clin. Chem.*, 2004, **50**, 2469-2470.
23. J. L. McHale, *Molecular Spectroscopy*, CRC Press, Boca Raton, 2017.
24. J. Sauther, J. Wusten, S. Lach and C. Ziegler, *J. Chem. Phys.*, 2009, **131**, 034711.
25. C. Adamo and D. Jacquemin, *Chem. Soc. Rev.*, 2013, **42**, 845-856.
26. M. Gruenewald, L. K. Schirra, P. Winget, M. Kozlik, P. F. Ndione, A. K. Sigdel, J. J. Berry, R. Forker, J. L. Bredas, T. Fritz and O. L. A. Monti, *J. Phys. Chem. C*, 2015, **119**, 4865-4873.
27. N. J. Hestand and F. C. Spano, *Chem. Rev.*, 2018, **118**, 7069-7163.
28. F. N. Xia, H. Wang, D. Xiao, M. Dubey and A. Ramasubramaniam, *Nat Photonics*, 2014, **8**, 899-907.
29. R. Forker, D. Kasemann, T. Dienel, C. Wagner, R. Franke, K. Mullen and T. Fritz, *Adv. Mater.*, 2008, **20**, 4450-4454.
30. M. Gruenewald, K. Wachter, M. Meissner, M. Kozlik, R. Forker and T. Fritz, *Org. Electron.*, 2013, **14**, 2177-2183.
31. M. Gruenewald, J. Peuker, M. Meissner, F. Sojka, R. Forker and T. Fritz, *Phys. Rev. B*, 2016, **93**, 115418.
32. M. Gruenewald, C. Sauer, J. Peuker, M. Meissner, F. Sojka, A. Scholl, F. Reinert, R. Forker and T. Fritz, *Phys. Rev. B*, 2015, **91**, 155432.
33. P. K. Nayak, *Synth. Met.*, 2013, **174**, 42-45.
34. P. K. Nayak and N. Periasamy, *Org. Electron.*, 2009, **10**, 1396-1400.
35. P. I. Djurovich, E. I. Mayo, S. R. Forrest and M. E. Thompson, *Org. Electron.*, 2009, **10**, 515-520.
36. O. H. Pakarinen, J. M. Mativetsky, A. Gulans, M. J. Puska, A. S. Foster and P. Grutter, *Phys. Rev. B*, 2009, **80**, 085401.
37. H. Aldahhak, W. G. Schmidt and E. Rauls, *Surf. Sci.*, 2013, **617**, 242-248.
38. R. Zacharia, H. Ulbricht and T. Hertel, *Phys. Rev. B*, 2004, **69**, 155406.
39. H. Sun, S. Ryno, C. Zhong, M. K. Ravva, Z. Sun, T. Korzdorfer and J. L. Bredas, *J Chem Theory Comput*, 2016, **12**, 2906-2916.
40. J. B. Neaton, M. S. Hybertsen and S. G. Louie, *Phys. Rev. Lett.*, 2006, **97**, 216405.
41. J. E. Norton and J. L. Bredas, *J. Am. Chem. Soc.*, 2008, **130**, 12377-12384.
42. N. Ueno and S. Kera, *Prog. Surf. Sci.*, 2008, **83**, 490-557.
43. S. Refaely-Abramson, S. Sharifzadeh, M. Jain, R. Baer, J. B. Neaton and L. Kronik, *Phys. Rev. B*, 2013, **88**, 081204.

44. S. Sharifzadeh, A. Biller, L. Kronik and J. B. Neaton, *Phys. Rev. B*, 2012, **85**, 125307.
45. A. Droghetti, I. Rungger, C. Das Pemmaraju and S. Sanvito, *Phys. Rev. B*, 2016, **93**, 195208.
46. J. M. Garcia-Lastra and K. S. Thygesen, *Phys. Rev. Lett.*, 2011, **106**, 187402.
47. R. Forker, M. Gruenewald and T. Fritz, *Annu. Rep. Prog. Chem., Sect. C: Phys. Chem.*, 2012, **108**, 34-68.
48. I. G. Hill, A. Kahn, Z. G. Soos and J. R. A. Pascal, *Chem. Phys. Lett.*, 2000, **327**, 181-188.
49. T. Graber, F. Forster, A. Scholl and F. Reinert, *Surf. Sci.*, 2011, **605**, 878-882.
50. W. R. Salaneck, *Phys. Rev. Lett.*, 1978, **40**, 60-63.
51. E. V. Tsiper, Z. G. Soos, W. Gao and A. Kahn, *Chem. Phys. Lett.*, 2002, **360**, 47-52.
52. H. Kubota, T. Munakata, T. Hirooka, K. Kuchitsu and Y. Harada, *Chem. Phys. Lett.*, 1980, **74**, 409-412.
53. S. Duhm, Q. Xin, S. Hosoumi, H. Fukagawa, K. Sato, N. Ueno and S. Kera, *Adv. Mater.*, 2012, **24**, 901-905.
54. M. Kytka, L. Gisslen, A. Gerlach, U. Heinemeyer, J. Kovac, R. Scholz and F. Schreiber, *J. Chem. Phys.*, 2009, **130**, 214507.
55. S. Duhm, A. Gerlach, I. Salzmann, B. Broker, R. L. Johnson, F. Schreiber and N. Koch, *Org. Electron.*, 2008, **9**, 111-118.
56. G. M. Rangger, O. T. Hofmann, L. Romaner, G. Heimel, B. Broker, R. P. Blum, R. L. Johnson, N. Koch and E. Zojer, *Phys. Rev. B*, 2009, **79**, 165306.
57. S. Kera, H. Yamane and N. Ueno, *Prog. Surf. Sci.*, 2009, **84**, 135-154.
58. M. L. Blumenfeld, M. P. Steele, N. Ilyas and O. L. A. Monti, *Surf. Sci.*, 2010, **604**, 1649-1657.
59. T. Ueba, J. Park, R. Terawaki, Y. Watanabe, T. Yamada and T. Munakata, *Surf. Sci.*, 2016, **649**, 7-13.
60. E. V. Tsiper and Z. G. Soos, *Phys. Rev. B*, 2001, **64**, 195124.
61. Z. G. Soos and E. V. Tsiper, *Macromol. Symp.*, 2004, **212**, 1-12.
62. A. Hauschild, R. Temirov, S. Soubatch, O. Bauer, A. Scholl, B. C. C. Cowie, T. L. Lee, F. S. Tautz and M. Sokolowski, *Phys. Rev. B*, 2010, **81**, 125432.
63. R. Forker, T. Dienel, A. Krause, M. Gruenewald, M. Meissner, T. Kirchhuebel, O. Gröning and T. Fritz, *Phys. Rev. B*, 2016, **93**, 165426.
64. S. Babar and J. H. Weaver, *Appl. Opt.*, 2015, **54**, 477-481.
65. I. Vragović and R. Scholz, *Phys. Rev. B*, 2003, **68**, 155202.
66. M. Hoffmann, K. Schmidt, T. Fritz, T. Hasche, V. M. Agranovich and K. Leo, *Chem. Phys.*, 2000, **258**, 73-96.
67. V. Bulović, P. E. Burrows, S. R. Forrest, J. A. Cronin and M. E. Thompson, *Chem. Phys.*, 1996, **210**, 1-12.